Prescribed Fire Monitoring Using KHawk Unmanned Aircraft Systems: Initial Flight Test Results

Saket Gowravaram[1], Harold Patrick Flanagan[2], Pengzhi Tian[3], Haiyang Chao [4]
University of Kansas, Lawrence, KS, 66045

Low-cost unmanned aircraft systems have become very popular remote and in-situ sensing platforms for many military and civilian applications. However, most small UASs operate in calm weather conditions at low flying speeds, which make their use limited in challenging disaster scenarios such as prescribed fires or wild fires. This paper provides preliminary flight test results for monitoring of a prescribed fire using fixed-wing KHawk UASs, including detection and analysis of fire line evolution and UAS turbulence responses. Aerial videos collected by KHawk UASs are orthorectified using the Structure from Motion (SFM) algorithm. Initial fire line extraction algorithm is proposed and validated using collected aerial images. Multiple metrics including body frame acceleration, vertical acceleration, and derived equivalent vertical gust velocity (EVG) are used for the detection of UAS turbulence encounters using collected UAS telemetry data.

Nomenclature

a_d = Vertical Acceleration
a_x = Body Acceleration in x-direction
a_y = Body Acceleration in y-direction
a_z = Body Acceleration in z-direction
p = Roll Rate
q = Pitch Rate
r = Yaw Rate
$\emptyset$ = Roll Angle
θ = Pitch Angle
ψ = Yaw Angle
α = Angle of Attack
β = Sideslip Angle
U_{de} = Equivalent Vertical Gust Velocity
V_a = True Airspeed
n = Load Factor
K_g = Factor to account for airplane motion
C_{L_α} = Lift Curve Slope
S = Wing reference area
W_n = North Wind speed
W_e = East Wind speed
W_d = Vertical Wind speed

[1]M.S. Student, Aerospace Engineering Department, University of Kansas, Lawrence, KS, 66045, (E): saket_aero@ku.edu.
[2]Ph.D. Student, Aerospace Engineering Department, University of Kansas, Lawrence, KS, 66045, (E): h682f304@ku.edu.
[3]Ph.D. Student, Aerospace Engineering Department, University of Kansas, Lawrence, KS, 66045, (E): pengzhitian@ku.edu.
[4]Assistant Professor, Aerospace Engineering Department, University of Kansas, Lawrence, KS, 66045, (E): chaohaiyang@ku.edu.

V_d = Down ground speed
V_n = North ground speed
V_e = East ground speed
W = Aircraft weight

I. Introduction

Prescribed or controlled burning of land is a technique used to create or maintain the desired vegetation or habitat conditions. Periodic fires are also known to reduce the chances of future wildfires by reducing fuel load. It is, however, important to monitor and control the propagation of prescribed fires for safety reasons. More importantly, the same techniques used for sensing, modeling, and prediction of prescribed fires can be adapted for more dangerous wildfires, which devastate thousands of hectares of land and crops each year. Apart from the destruction of habitat and biodiversity, wildfires generate a large number of human causalities each year, making firefighting activities extensively risky. However, it is very difficult to have an accurate operational wildfire spread model due to the non-linear nature of fire propagation and fire-atmospheric coupling.

The behavior of wildfires can be affected by factors such as fuel characteristics, weather, and topography [1]. Weather conditions like humidity and winds have a big impact on the direction and speed of fire propagation. For example, winds increase the fire propagation speed along the wind direction and the relative humidity influences the intensity of the flames and extent of fire damage. Wildfire monitoring involves real-time estimation of important fire parameters including location and shape of the fire front, rate of propagation of fire line and the maximum height of the flames [2]. These parameters can be used by firefighters for more effective and safer firefight planning. However, the estimations of these parameters by ground visual inspection may not be accurate. Instead, different remote sensing platforms such as satellite and manned aircraft have been used for firefighting.

Wildfire remote sensing platforms have been traditionally used for fire impact quantification, vegetation recovery tracking, fuel conditions establishment and fire detection. They are increasingly used for real time fire monitoring due to the improvement in sensing accuracy and resolution. Satellite sensor platforms such as Landsat Thematic Mapper (TM), Moderate Resolution Imaging Spectroradiometer (MODIS) and Landsat Multispectral Scanner (MSS) with ground resolutions of 30 m – 1 km have been used in wildfire remote sensing applications [3]. However, due to low frequency and constrained image resolution, these methods are restricted to just coarse fire detection and post-fire burn mapping. Manned aircraft is also widely used for fire monitoring and suppression. However, it is very dangerous to operate in fire fields, which is highly turbulent. Shorter response time, higher resolution and automatic navigation capabilities have made UAS based fire monitoring an important and popular approach in recent years.

A single UAS or multiple UASs have been successfully used for fire monitoring and observation as shown in [4, 5]. An automatic real-time forest fire monitoring technique using several UASs with on-board infrared or visual cameras and a central station was proposed and valdiated [6]. Casbeer et al. [7] developed an effective path planning algorithm using infrared images which are procured from the on-board camera for simulated forest fire boundary following. The use of multiple cooperative Low-altitude short endurance (LASE) UAVs for fire monitoring has been investigated [8], by using service agent UAVs and detection agent UAVs (fire detection and communication with service agent UAVs). Ononye et al. [9] utilized the Dynamic Data Acquisition system to determine fire perimeter, fire line and fire propagation direction with the help of multispectral aerial imagery. UASs have also been used to ignite fires as a part of wildfire suppression tactics [20]. The inclusion of high-quality thermal sensors on UASs can improve fire monitoring capabilities as demonstrated by Project FiRe in 2001 [4]. The experiment conducted by Ambrosia et al. [4] presents the use of thermal multispectral scanning imager integrated on a UAV, a satellite uplink/downlink image data telemetry system, and near real-time geo-rectification techniques for robust fire monitoring. UASs can also be deployed for simultaneous search and rescue operations in forest fires due to their real-time communication capability with control centers, ground stations and other manned and unmanned aircraft [10]. Prompt and robust fire detection requires high accuracy fire data and efficient computer vision algorithms for fire detections. Martinez-de Dios et al. [11] demonstrated the use of visual and infrared cameras with telemetry sensors and GPS for forest fire perception. With the use of a 3D perception model and sensor fusion techniques, they can provide important forest fire estimates including fire front, flame height, flame inclination angle and fire base width. A state of the art vision-based fire and smoke detection algorithm was developed by Verstockt et al. [12], which is based on a chromatically-based background subtraction method with back-step correction, wavelet-based energy analysis, and boundary disorder analysis. A combination of these advanced fire detection algorithms and efficient UASs can be highly effective in achieving fast and accurate fire analysis. However, there exist many challenges that need to be addressed before routine deployment of UASs for real-time monitoring of prescribed or wild fires.

Fires can greatly alter the weather and atmospheric conditions due to high temperature. The heat and moisture produced by the fire change the temperature of the surroundings, and create intense winds including strong updrafts or downdrafts [1]. Such instabilities and drastic changes in the atmosphere can cause severe turbulence. UASs, being lighter and closer to the ground, are more vulnerable to these drastic and dynamic flows than manned aircraft. Therefore, the flight performance of small UASs in such conditions need to be analyzed first in order to achieve safe and efficient monitoring of prescribed or wildfires.

This paper aims to address some of the important aspects of UAS-based fire remote sensing including the development of a low-cost UAS and associated algorithms for fire line detection using RGB cameras. The flight response of the aircraft above the fires is analyzed using onboard telemetry from pressure, inertial and GPS sensors.

The organization of this paper can be summarized as follows. Long-term objectives of UAS-based fire remote sensing and the current problem definition of this paper are presented in Section II. Section III focuses on descriptions of the prescribed fire and the UAS sensing platforms used for this project. Section IV represents the approach used for vision-based sensing of the fire followed by UAS turbulence sensing in Section V. Finally, conclusions and future work recommendations are mentioned in section VI.

II. Long-Term Objective & Problem Definition

The long term objective of UAS-based fire monitoring is to provide real-time fire data for operational wildfire spread modeling and prediction. Reliable and accurate predictions of wildfire spreading requires real-time fire line data with high spatial and temporal resolutions (e.g., ~10 m and 10 min for local-scale fires) [13]. UAS has big potentials to provide such information in these dangerous environments. However, it is very challenging to fly manned or unmanned aircraft in fire burning fields because of strong turbulence generated by the fire-atmosphere coupling.

The objective of this paper is to perform initial evaluations of using small UASs for fire monitoring missions. Two subtasks are focused including estimation of fire line location and evolution, and analysis of UAS turbulence encounter data for future small UAS operations. Photogrammetric procedures using the SFM algorithm are used for mapping the area of interest before and after fire burning based on collected aerial videos. Additionally, images obtained from the UAS during the fire burning are classified to distinguish the fire line, burnt areas and unburnt areas. The information procured from the on-board inertial, pressure and GPS sensors are used to estimate the fluctuations in vertical accelerations and estimate the vertical gust velocity and vertical winds. The identified turbulence response periods are validated through visual data obtained from the camera.

III. Prescribed Fire and UAS Sensing Platform

A prescribed fire was organized by the Kansas Biological Survey (KBS) crew at the KU field station as a routine method for controlling the vegetation. The burned area is about 350 × 170 meters. It was burned from 10:56 to 11:38 AM on April 7th, 2017. The wind was about 7 mph from the south. A mower was used to create a fire insulation strip several weeks before the burn. The fire was started as a ring fire pattern. The KBS crews started from the north of the field at around 10:56 AM and finished the circle at the south at around 11:30 AM. The approximate start time of the fire is estimated based on the first sighting of fire/smoke on the video from the on-board camera on the first flight. Its corresponding frame is extracted and is referenced with GPS and IMU data. With the knowledge of take-off time from flight log and the global time data (ITOW) from GPS, the approximate fire start time is calculated. The end time is calculated based on the first sighting of dying fire/smoke from the aerial video collected in the second flight. Detailed temporal information for the prescribed fire can be found in Table 1.

Table 1. Temporal characteristics of fire.

Description	Time
Fire Start Time	10:56:59 AM (CST)
Full Intensity Fire Time	11:32:44 AM (CST)
Fire End Time	11:38:06 AM (CST)
Approximate Duration of Fire	41 minutes 7 sec

Two UASs were used for fire sensing including a KHawk 48” UAS and a KHawk 55”UAS. KHawk UASs were developed by researchers in the Cooperative Unmanned Systems Laboratory (CUSL) at the University of Kansas (KU). Table 2 represents the detailed specifications of these aircraft.

Table 2. KHawk UAS specifications.

Description	KHawk 48”	KHawk 55”
Takeoff Weight	3.8 lbs.	5.5 lbs.
Wing Span	48 in.	55 in.
Cruise Speed	20 m/s	20 m/s
Flight Time	≤ 30 minutes	≤ 45 minutes
Sensing Payload	GPS, Inertial Sensors, GoPro Hero 4	GPS, Inertial Sensors, GoPro Hero 4, Eagle Tree Pressure Sensor

KHawk 48” UAS (Figure 1) is a flying wing aircraft made from EPP foam with a wingspan of 48”. The aircraft is powered by a pusher-type propeller and an electric brushless motor. It has two elevons as the control surfaces for roll and pitch control, shown in Figure 1. The takeoff weight is approximately 4 lbs including payloads. Three 11.1V 2000 mAh batteries are used to power, which can support up to 30 minutes of flight with the payload. KHawk 48” UAS is equipped with a Microstrain GX3 IMU, a Ublox-Lea 6h GPS receiver, and a Paparazzi autopilot, which can support both manual or autonomous flight modes. A modified GoPro Hero 4 camera was installed on the belly of the aircraft looking downward.

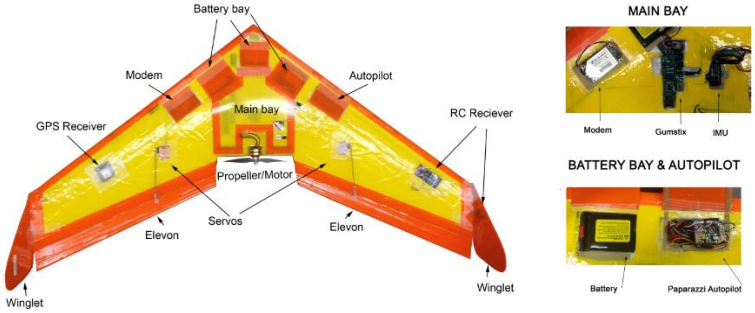

Figure 1. KHawk 48” UAS.

KHawk 55” UAS (Figure 2) is a flying wing aircraft made from EPOR foam with a wingspan of 55”. It is equipped with similar avionics with KHawk 48”, which can support autonomous GPS waypoint tracking as well. A pitot-tube system (dynamic pressure) was installed for data collection. All the sensor data is logged onboard the aircraft including inertial data (100 Hz), GPS data (4 Hz), and airspeed data (50 Hz). Six 11.1V 2000 mAh batteries are used to power, which can support up to 60 minutes of flight with the minimal takeoff weight.

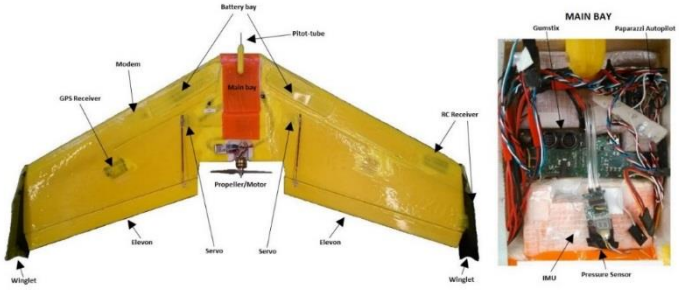

Figure 2. KHawk 55” UAS.

A modified PeauPro82 GoPro Hero 4 Black Camera was used for aerial video acquisition onboard KHawk UAS 48” and KHawk UAS 55”. The fisheye lens was replaced with a 3.97mm lens with minimal radial distortions. The camera specifications are mentioned in Table 3.

Table 3. Camera specifications.

Description	Value
Focal Length (mm)	3.97
Weight (g)	90
Angle Of View (VxHxD) (°)	65×82×92
Aperture	2.8
Back Focal Length (mm)	4.65
Dimensions (Diameter x Length) (mm)	17.40 × 22.48 mm
Resolution Mode	1920 × 1080 p

A total of three flights were conducted at the KU field station to observe the field before, during and after the fire. A brief descriptions of these flights are provided in Table 4.

Table 4. Flight descriptions.

UAS	Flight Time	Flight Mode/Height	Raw Sensor Outputs	Update Rates(Hz)
KHawk 48 UAS (1st Flight)	10:54 AM – 11:06 AM	Autonomous/ 100-120m	$a_x/a_y/a_z, p/q/r, \emptyset/\theta/\psi$	100
			x/y/z, $V_n/V_e/V_d$	4
KHawk 55 UAS (2nd Flight)	11:28 AM-11:38 AM	Manual / 40m-114m	$a_x/a_y/a_z, p/q/r, \emptyset/\theta/\psi$	100
			x/y/z, $V_n/V_e/V_d$	4
			V_a	50
KHawk 48 UAS (3rd Flight)	11:58 AM – 12:15 AM	Autonomous/ 100-120m	$a_x/a_y/a_z, p/q/r, \emptyset/\theta/\psi$	100
			x/y/z, $V_n/V_e/V_d$	4

IV. Vision Sensing of Fire Burning

The objective for vision sensing of fire burning sites is to detect the location of the fire line at specified spatial and temporal resolutions. Two approaches can be employed, area sweeping method or fire line following method. The area sweeping method is to sweep the selected burning area at required temporal resolutions. The fire line following method is to detect and follow the fire lines reactively. The area sweeping algorithm is easy to implement. However, it only works for small burning areas such as certain prescribed fires. Fire line following approaches are better suited for general wildfire tracking. However, it requires more efforts in algorithm development and implementation. After the acquisition of the aerial images and the generation of orthorectified maps, image processing algorithms can be used for the detection of the fire line location, burnt areas, and unburnt areas. A simple image classification algorithm is developed in this paper for RGB images while similar strategies can be used for infrared images. An RGB image can be separated into three individual bands, Red, Green and Blue ($dn_R/dn_G/dn_B$) expressed in digital numbers. The R band can be used to detect the fire line location, burnt region and unburnt region based on its reflectance range. Considering different R reflectance values of the surfaces (burnt, unburnt and fire line), thresholds $DN_{R,F}$ and $DN_{R,B}$ can be defined, which denote the minimum R reflectance value of the fire and maximum R reflectance value of the burnt region. The overall algorithm can be summarized as:

$$Fireline: dn_R > DN_{R,F},$$
$$Unburnt\ Area: DN_{R,B} > dn_R > DN_{R,F},$$
$$Burned\ Area: dn_R < DN_{R,B}.$$

Initial flight tests focused on the global mapping (350 × 170 m) of the fire field in the beginning and after the fire burning as well as fire line detection using local aerial images (~50 × 40 m) during the fire burning. The flight trajectories of the KHawk 48" and KHawk 55" UASs which were flown before and during the fire are shown in Figure 3 and Figure 4 respectively. The area bound by the red path is the area which was subject to the prescribed fire. It can be observed that the KHawk 48" UAS maintained predefined lines and circles in auto mode and was able to cover the entire subject area, as compared to the KHawk 55" UAS. Small course oscilation can be observed in the KHawk 48" flight path because the UAS flew with or into the wind (~5 m/s). The KHawk 55" flight path was expected since the

it was flown manually over smoke areas above the fire as mentioned in Table 4. A total of 47 images was selected and used for the stitching and georeferencing out from 15,747 image frames collected during the 1st flight. AgiSoft Professional software was used for the offline stitching and othorectification. The final orthomosaic map is shown in Figure 5, which has a ground resolution of 10.8 cm/pix. KHawk 48" UAS was flown after the burning as well. A total of 50 images was used for the stitching. The final orthomosaic map is shown in Figure 6 which has a ground resolution of 10.5 cm/pix. The fire region classification algorithm is tested using the final stitched aerial maps, which are shown in the right parts of Figures 5 and 6. It can be observed that the algorithm can detect most of the burnt and unburnt areas.

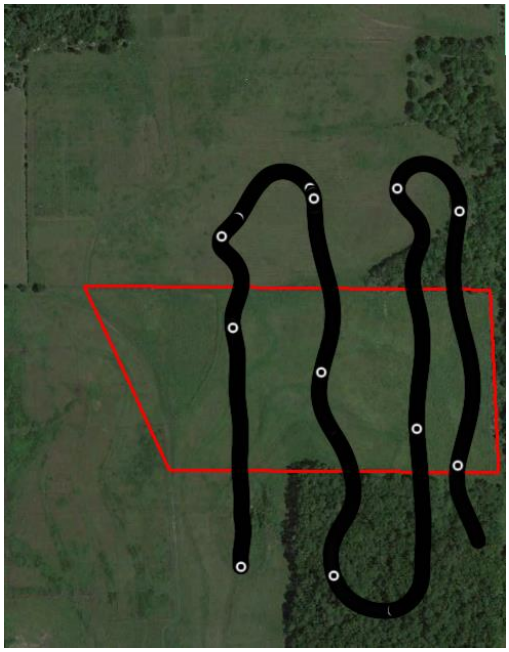

Figure 3. KHawk 48" flight trajectory.

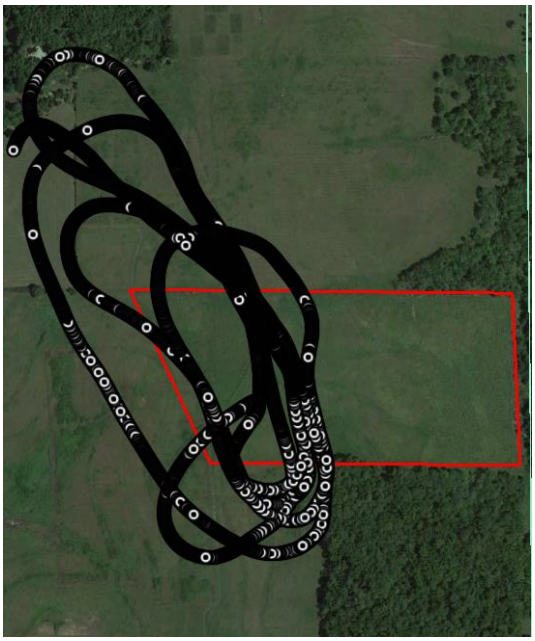

Figure 4. KHawk 55"flight trajectory.

Figure 5. RGB aerial map and burnt region (white) from KHawk 48" UAS 1st flight.

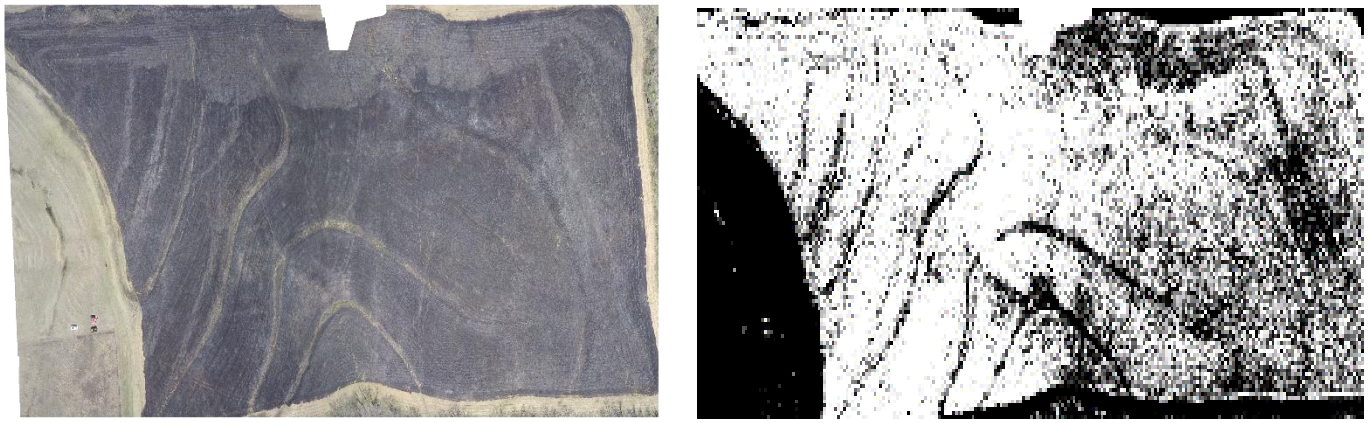

Figure 6. RGB aerial map and burnt region (white) KHawk 48" UAS 3rd flight.

The classification algorithm was also applied to individual aerial image frames which were acquired from the KHawk 55" flight during the fire burning as shown in **Error! Reference source not found.**-10 representing the fire line, unburnt area and burnt area respectively.

Figure 7. RGB aerial image.

Figure 8. Extracted fire line.

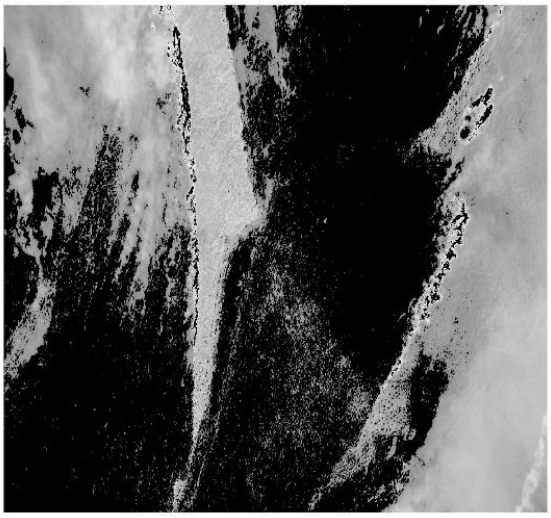

Figure 9. Unburnt area.

Figure 10. Burnt area.

It can be observed that the algorithm works well in detecting the fire line in individual images as well as constructed orthomosaic maps and therefore forms the basis of a real-time UAS path planning algorithm.

In summary, the flight trajectory of the UAS plays a vital role in the estimation of the spatial and temporal characteristics of the fire. Given aircraft parameters such as cruise speed, altitude and endurance coupled with the characteristics of the imaging sensor, an effective flight trajectory can be generated. Once, in the air, the fire line detection algorithm presented in this section can be used to navigate the UAS in real time based on the propagation of fire. With real time estimation of the fire speed and direction, the flight speed, course and altitude can also be changed to ensure maximum observation of the fire.

V. Turbulence Sensing

The objective for turbulence sensing is to quantify the UAS performance and flight risks while flying in strong fire generated turbulence. The problem can be described as the quantification of UAS turbulence responses based on pressure (V_a,α,β), inertial ($p/q/r$, $a_x/a_y/a_z$,$\emptyset/\theta/\psi$) and GPS (x/y/z,$V_n/V_e/V_d$) measurements. There are generally two ways to quantify aircraft turbulence responses, through wind based metrics or aircraft based metrics. The metrics which have been used for flight investigation of turbulence responses from manned aircraft include body frame acceleration, vertical acceleration, equivalent vertical gust velocity (EVG), vertical wind velocity, and eddy dissipation rate (EDR) [15, 16, 17]. In this paper, we investigated the use of body frame acceleration, vertical acceleration, EVG and vertical wind velocity to quantify the turbulence response experienced by the aircraft. Images acquired by the on-board camera are used to correlate the trends observed in these metrics and thereby justify the effects of smoke and fire on the aircraft.

Vertical acceleration is a major indicator for turbulence encounters of passenger aircraft. For manned aircraft, vertical acceleration and body z acceleration are similar. Similar assumptions may not work for small UASs. The vertical acceleration can be calculated from the body accelerations and aircraft orientation information as shown below [17]:

$$a_d = \cos\emptyset\cos\theta\, a_z + \sin\emptyset\cos\theta\, a_y - \sin\theta\, a_x + \text{g}. \quad (1)$$

In addition to the vertical acceleration, other parameters such as the equivalent vertical gust velocity and vertical wind velocity can also be calculated in order to quantify the turbulence. Wind based metrics can be easily used by other aircraft with different flight specifications in the same airspace. During wings level steady state flight, the equivalent vertical gust velocity is defined as the change in angle of attack, α times the aircraft forward speed V_a as shown below [18]:

$$U_{de} = \Delta\alpha V_a. \quad (2)$$

A vertical gust can cause an instantaneous change in lift and therefore a change in the load factor, *n.* This change can be mathematically formulated as follows:

$$\Delta n = \frac{K_g U_{de} V_a C_{L_\alpha} S}{498W} . \quad (3)$$

The vertical wind W_d can be calculated from the measurements from the inertial sensors and on-board air data system such as a 5-hole pitot tube or a routine pitot tube with angle vanes using basic wind triangular rules. The equation is shown below [16]:

$$W_d = V_a(\cos\emptyset\cos\theta\sin\alpha\cos\beta + \sin\emptyset\cos\theta\sin\beta - \sin\theta\cos\alpha\cos\beta) - V_d \quad (4)$$

When the sideslip angle is small, the above equation can be simplified as the following:

$$W_d = V_a(cos\theta sin\alpha cos\emptyset - cos\alpha sin\theta) - V_d \quad (5)$$

(4) and (5) are easy to implement, however, they require accurate aircraft attitude and flow angle measurements. It is also possible to use estimated angles of attack and sideslip for calculations of wind velocities.

The KHawk 55" UAS flight data are used for turbulence quantification because it flew into fire generated smokes multiple times. As a reference, the 3-D ground wind measurements acquired from the KU Weather station is presented below, which is about 200 meters north of the burning field. **Error! Reference source not found.** and Figure 12 represent the raw measurements and filtered (moving average with 20s window) estimation of the wind respectively. A model-aided extended Kalman filter is developed for simultaneous estimation of aircraft flow angles and wind speeds based on collected inertial, pressure, and GPS data [19], as shown in Figure 13. Although the UAS estimated wind velocities match the overall trend of weather station data, the high frequency turbulence component may already be filtered out due to wind model inaccuracy. Therefore, direct analysis of UAS telemetry data is needed.

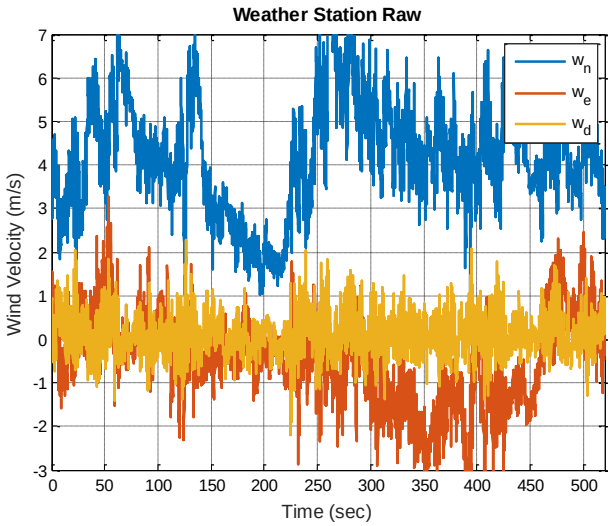

Figure 11. 3-D Wind measurement from weather station (Raw).

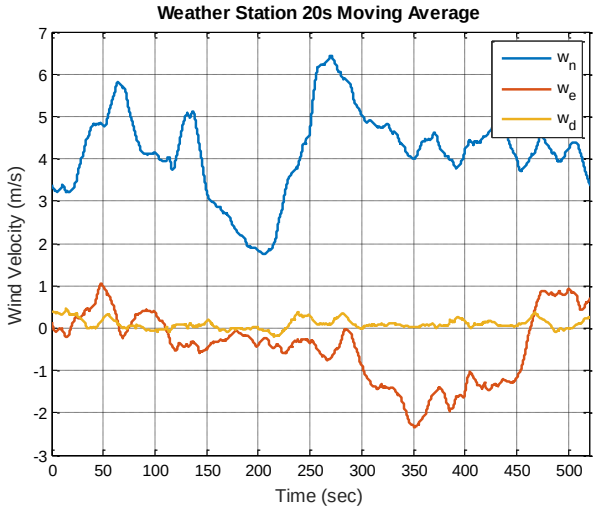

Figure 12. 3-D Wind measurement from weather station (Moving average filter with 20s window).

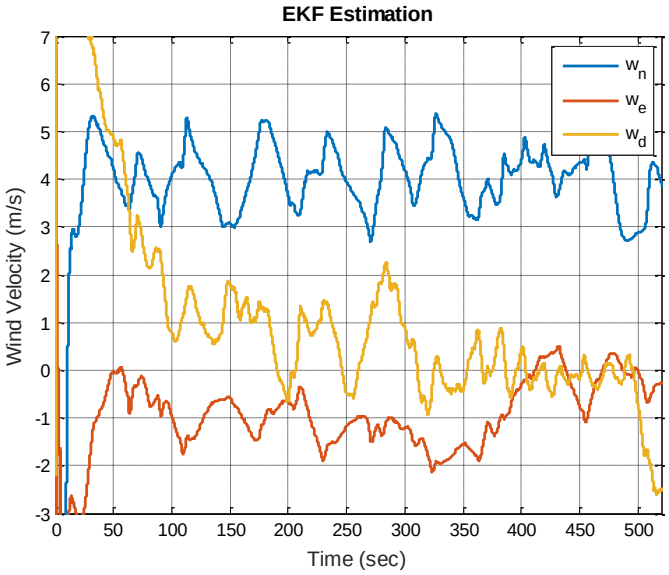

Figure 13. Model aided estimation of 3-D winds [19].

The body acceleration (Figure 14) and angular rates (Figure 15) were first analyzed to identify if any unstable mode of the aircraft was triggered. It was observed that the Dutch Roll mode of the KHawk 55" was activated during the fire flight. The frequency of the Dutch Roll appears to be about 1 Hz. The turbulence from the fire caused this mode to be activated which requires immediate pilot intervention. It is envisioned that a flight autopilot can potentially react and compensate for disturbances at this frequency after adding this disturbance in the controller design specifciations.

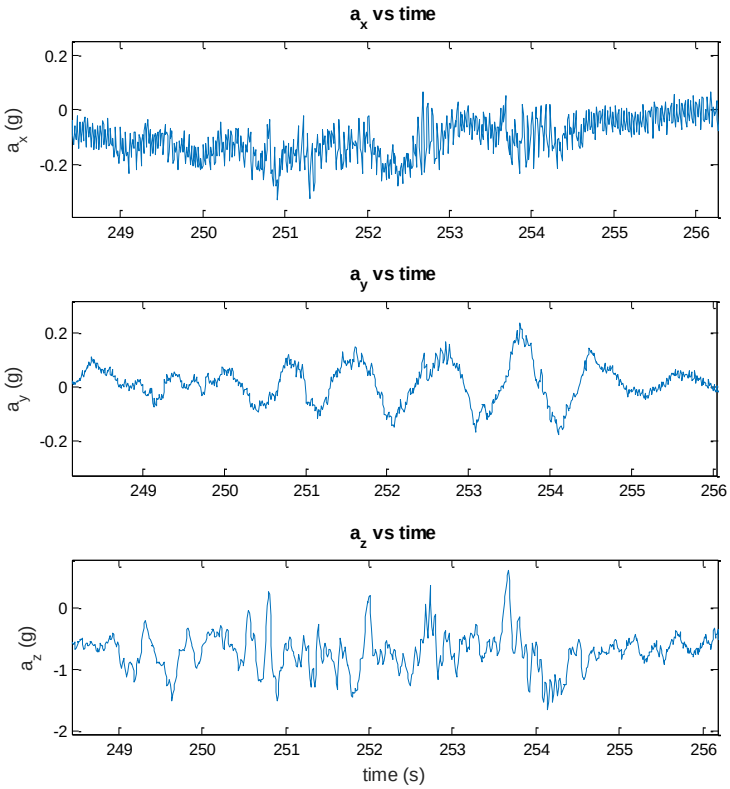

Figure 14. Body accelerations during Dutch Roll.

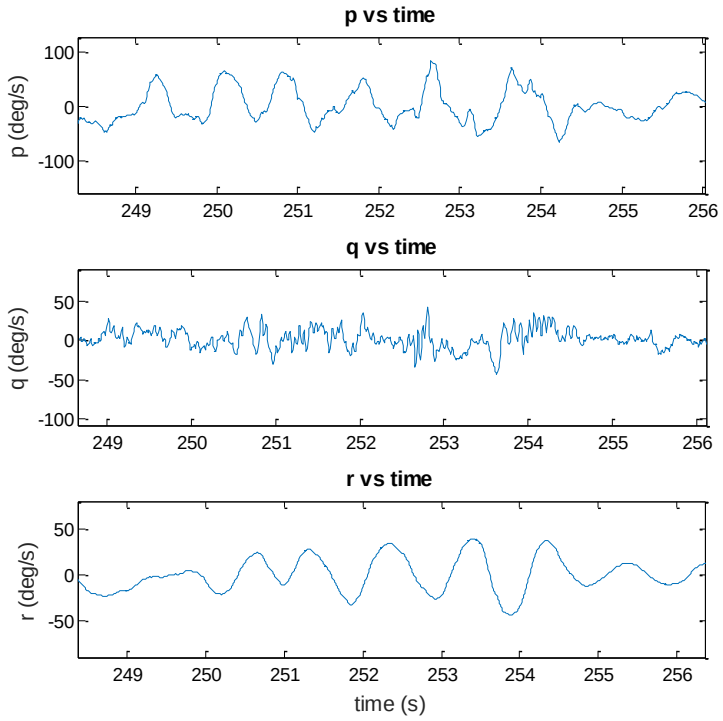

Figure 15. Angular rates during Dutch Roll.

The second investigation is to detect turbulence encounters based on vertical accelerations. Multiple turbulence encounters were observed during the KHawk 55" flight. This can be seen by the increase in the vertical acceleration as shown in Figure 16.

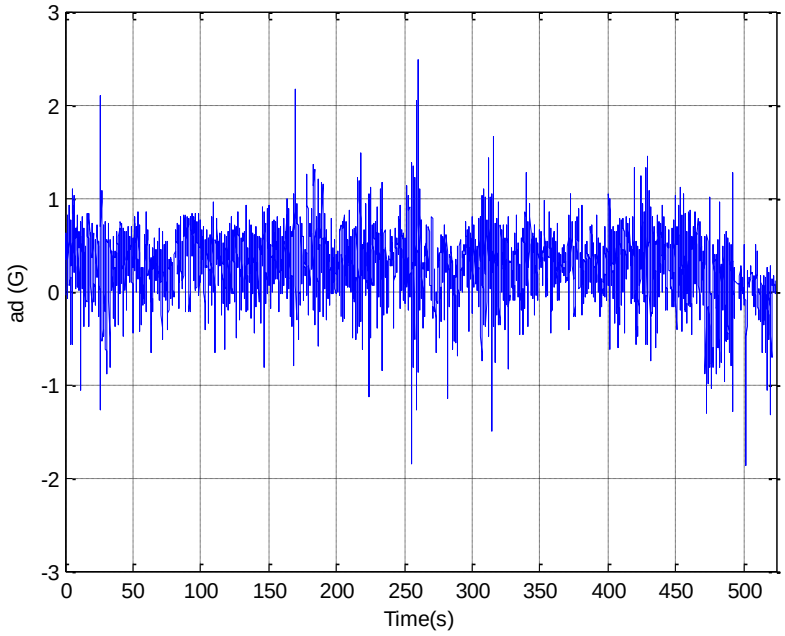

Figure 16. KHawk 55" vertical acceleration data.

An increase of over 2 g's is noticeable during the most violent portion of the turbulence encounter. Thresholds for severe (bigger than 1 G) and moderate (bigger than 0.5 G) turbulence were defined and plotted against the nominal vertical acceleration data for this portion as shown in Figure 17. The global turbulence plot overlayed on nominal vertical acceleration is shown in Figure 18.

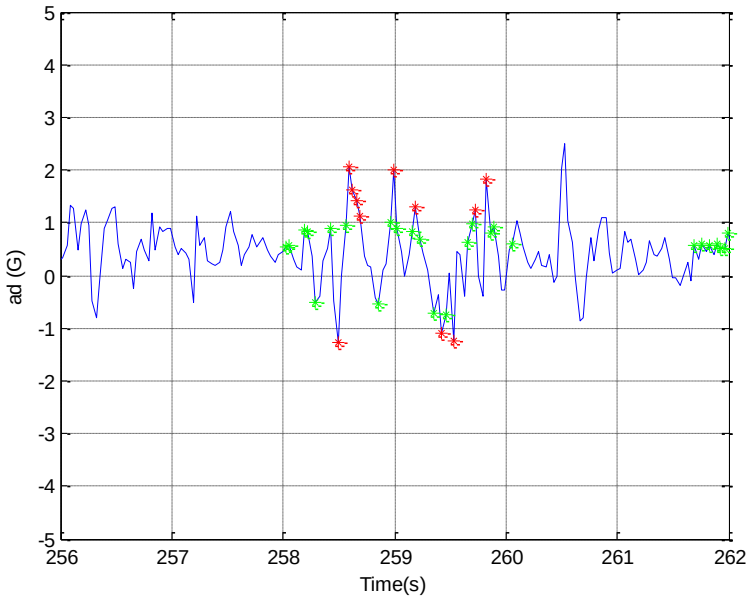

Figure 17. KHawk 55" vertical acceleration data during high turbulence encounters.

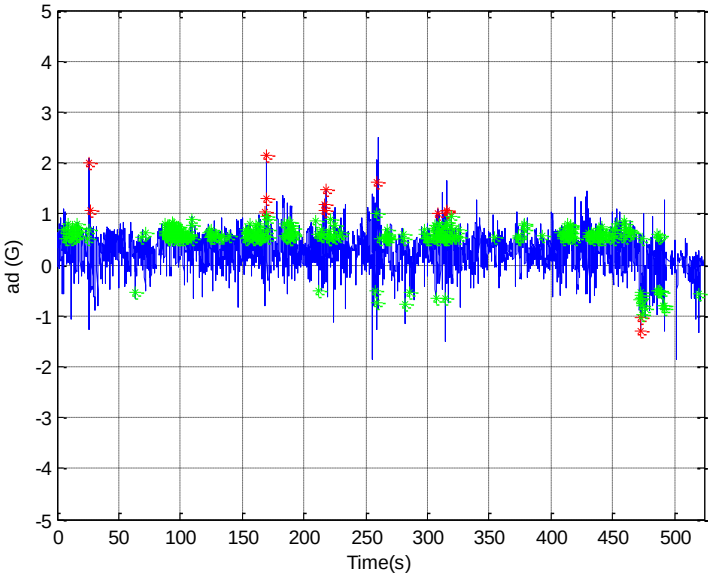

Figure 18. KHawk 55" turbulence data during the entire flight.

The flight path of the KHawk 55" UAS along with its turbulence is shown in **Error! Reference source not found.** It can be observed that the aircraft experiences most of its turbulence while flying over the region of fire. Turbulence is also observed when the aircraft was flying in the north boundary of the burning site, which can be attributed to the south winds as observed in Figure 13. Since the wind velocity is the strongest towards the north, it can be observed in the aerial video that the smoke from the fire moves to the north thereby creating some turbulence. However, further analysis needs to be made to draw solid conclusions.

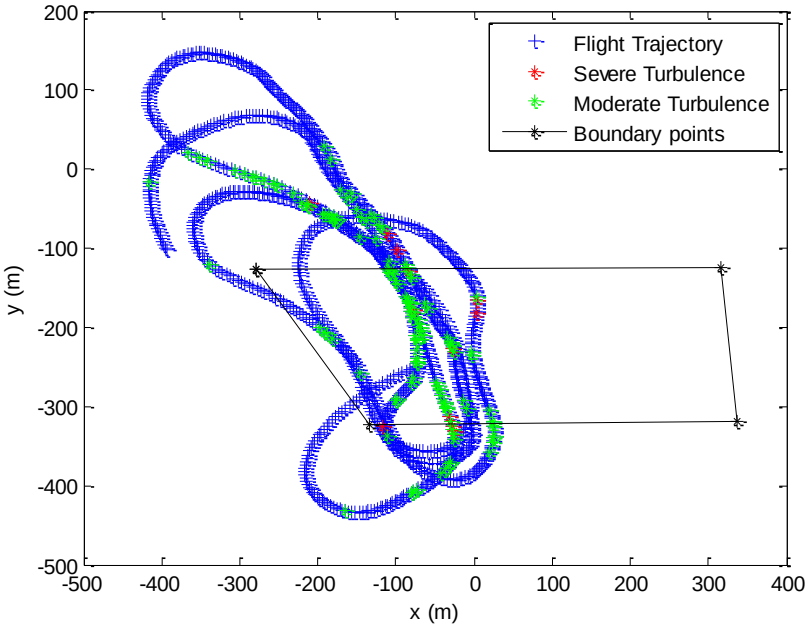

Figure 19. Flight path during turbulence.

It can be seen from Figure 17 that the aircraft was maintaining steady level flight right before the peaks are observed. It is expected the aircraft flew over thick smoke and intense fire which could justify the sudden jumps in vertical acceleration. Images were extracted at these exact times and locations as shown Figure 20. The images indicate presence of heavy smoke at these locations which justify the peaks observed in the aircraft's vertical accelerations. It is as predicted that flying directly over the smoke at low altitudes results in strong turbulence which sometimes make the aircraft very difficult to control.

Figure 20. Aerial images at points of severe turbulence.

A third investigation is to check the EVG values.The equivalent vertical gust velocity were plotted as shown in Figure 21 respectively. The angle of attack is estimated by an EKF based mainly from aircraft responses [19]. It can be observed that EVG showed similar trends with vertical acceleration.

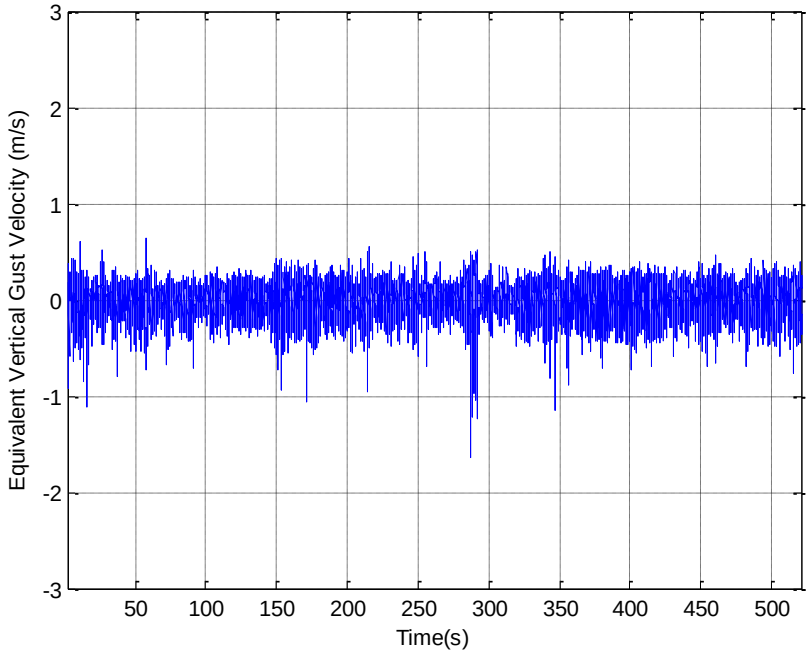

Figure 21. KHawk 55" Equivalent vertical gust velocity.

Strong correlations were observed among all the metrics during turbulence encounters. It can be concluded that flying over scattered smoke above the fire can cause some instabilities. However, it is manageable by the UAS remote pilot. If the aircraft were made to fly autonomously through large amounts of smoke, a robust controller may be needed to protect the aircraft against the fire generated turbulence. Understanding the behavior of the aircraft due to encounter with smoke forms an integral part of future fire monitoring flight planning.

Based on the trends observed in the aircraft behavior due to smoke-induced turbulence, the following recommendations can be made for future fire flight experiments.

1) Flying over the most intense part of fire can be avoided to prevent loss of aircraft control due to severe updrafts.
2) Other smoke areas can be flown into, however, the excitation of unstable modes (Dutch roll, spiral) might be triggered.
3) A safe flying altitude needs to be maintained.

VI. Conclusions

In summary, two different UASs were flown with various sensing payloads before, during and after a prescribed fire successfully. The CUSL researchers and KBS researchers work seamlessly for both fire burning and UAS flight testing while maintaining the safety. Initial aerial maps showed the potential of using small UASs for real-time detection of fire line evolution. Strong turbulence can be observed that can affect small UAS flight performance.

The following recommendations are made based on the experiences learned:

1) One UAS flight can be added 30 minutes before the burning to get the field map, wind and temperature data;
2) KHawk 48" UAS can be flown during the fires if not directly above the final center smoke;
3) The UAS needs to be further tuned and observed in different wind conditions so that the turbulence effect created by the fires can be singled out;
4) A temperature sensor with faster response time is needed for the temperature profile mapping;
5) A thermal camera can be added for more accurate detection and mapping of fire line evolution.

Acknowledgments

This work was partially supported by NASA-KS-EPSCoR grant NNX15AK36A R51438-2 and R51357-5. The authors would like to thank Dr. Nathaniel A. Brunsell for providing weather station data; Dr. Dean Kettle, Bruce Johanning, Vaughn Salisbury and other researchers from Kansas Biological Survey for helping with prescribed fire tests.

References

[1] Wildfire Modelling", [https://en.wikipedia.org/wiki/Wildfire_modeling].
[2] Viegas, D, "Forest Fire Monitoring", Philosophical Transactions: Mathematical, Physical and Engineering Sciences, Royal Society (pp. 2907-2928), 1998.
[3] Wing, M.G., Burnett, J., Sessions, J., "Remote Sensing and Unmanned Aerial System Technology for Monitoring and Quantifying Forest Fire Impacts", International Journal of Remote Sensing, 4(3), 113-120, 2014.
[4] Ambrosia, V., Wegener, S., Sullivan, D., Buechel, S., Brass, S.D.J., Stoneburner, J., Schoenung, S., "Demonstrating UAV-Acquired Real-Time Thermal Data over Fires", Photogrammetric Engineering and Remote Sensing, 69(4), 391-402, 2003.
[5] Maza, I., Caballero, F., Capitan, J., de Dios, J.M., Ollero, A., "Experimental results in multi-UAV coordination for disaster management and civil security applications", Journal of Intelligent and Robotic Systems, 61(1), 563-385, 2011.
[6] Merino, L., Caballero, F., de Dios, J.M., Maza, I., Ollero, A., "An Unmanned Aircraft System for Automatic Forest Fire Monitoring and Measurement", Journal of Intelligent and Robotic Systems, 65(1-4), 533-548, 2012.
[7] Casbeer, D., Beard, R., Li, S., McLain, T., Mehra, R.K., "Forest Fire Monitoring with Multiple Small UAVs", In IEEE American Control Conference, 2005.
[8] Sujit, P.B., Kingston, D., Beard, R., "Cooperative Forest Fire Monitoring Using Multiple UAVs". In IEEE Conference on Decision and Control, 2007.
[9] Ononye, A.E., Vodacek, A., Saber, E., "Automatic Extraction of fire line parameters from multispectral infrared images", Remote Sensing of Environment, 179-188, 2006.
[10] Karma, S., Zorba, E., Pallis, G.C., Statheropoulos, G., Balta, I., Mikedi, K., Vamvakari, J., Pappa, A., Chalaris, M., Xanthopoulos, G., Statheropoulos, M., "Use of unmanned vehicles in search and rescue operations in forest fires: Advantages and limitations observed in a field trial", International Journal of Disaster Risk Reduction, 207-312, 2015.
[11] De Dios, J.M., Arrue, B.C., Ollero, A., Merino, L., Gomez-Rodriguez, F., "Computer vision techniques for forest fire perception", Image and Vision Computing, 26, 550-562, 2008.
[12] Verstockt,S., Lambert, P., Van de Walle, Rik., Merci, B., Sette, B., "State of the art in vision-based fire and smoke detection", International Conference on Automatic Fire Detection, 285-292, 2009.
[13] Gollner, M., Trouve, A., Altintas, I., Block, J., Callafon, D., Clements, C., Cortes, A., Ellicott, E., Filippi, J.B., Finney, M., Ide, K., Jenkins, M.A., Jiminez, D., Lautenberger, C., Mandel, J., Rochoux, M., Simeoni, A., " Towards Data-Driven Operational Wildfire Spread Modelling", Report of the NSF-Funded Wildfire Workshop, 2015.
[14] Yuan, C., Ghamry, K.A., Liu, Z., Zhang, Y., "Unmanned Aerial Vehicle Based Forest Fire Monitoring and Detection Using Image Processing Technique", In IEEE Chinese Guidance, Navigation and Control Conference, 2016.
[15] Lemone, M.A., Pennell, W.T., "A Comparison of Turbulence Measurements from Aircraft", Journal of Applied Meteorology, 1980.
[16] Meymaris, G., Sharman, R., "NCAR In Situ Vertical winds-based EDR Estimation Algorithm", University Corporation for Atmospheric Research (UCAR), 2013.
[17] Beard, R. W., and McLain, T. W., "Small unmanned aircraft: Theory and practice", Princeton university press, 2012.
[18] Hoblit, F.M., "Gust Loads on Aircraft: Concepts and Applications", AIAA Education Series, 1988.
[19] Tian, P., Chao, H., "Model Aided Estimation of Angle of Attack, Sideslip Angle, and 3D Wind without Flow Angle Measurements", To appear in AIAA Guidance, Navigation and Control Conference, 2018.
[20] Twidell, D., Allen, C.R., Detweiler, C., Higgins, J., Laney, C., Elbaum, S., "Smokey come of age: Unmanned aerial systems for fire management", Frontiers in Ecology and the Environment, 14(6), 333-339, 2016.